

DIGIT Pinki: Using Fiber Optic Bundles to Miniaturize Vision-Based Tactile Sensors

Julia Di*, Zdravko Dugonjic†, Will Fu*, Tingfan Wu‡, Romeo Mercado‡, Kevin Sawyer‡,
Victoria Rose Most‡, Gregg Kammerer‡, Stefanie Speidel§, Richard E. Fan*, Geoffrey Sonn*,
Mark R. Cutkosky*, Mike Lambeta‡, and Roberto Calandra†

*Stanford University, Stanford, California, USA; Email: {juliadi, jiaxiang, refan, gsonn, cutkosky}@stanford.edu

†Technische Universität Dresden, Dresden, Germany; Email: {zdugonjic, rcalandra}@lasr.org

‡Meta, Menlo Park, California, USA; Email: {romeo12, kevin.sawyer, tingfan, victoriamost, gregk, lambetam}@meta.com

§National Center for Tumor Diseases (NCT/UCC) Dresden; Email: {stefanie.speidel}@nct-dresden.de

Abstract—Vision-based tactile sensors have recently become popular due to their combination of low cost, high spatial resolution, and ease of integration using widely available miniature cameras. The associated field of view and focal length, however, are difficult to package in a human-sized finger. This work uses optical fiber bundles to achieve a form factor that, at 15 mm diameter, is smaller than an average human fingertip. The electronics and camera are also located remotely, further reducing package size. The sensor achieves a spatial resolution of 0.22 mm and a minimum force resolution of 5 mN for normal and shear contact forces. With these attributes, the DIGIT Pinki sensor is suitable for applications such as robotic and teleoperated digital palpation. Its utility is demonstrated for a prostate cancer palpation use, achieving clinically relevant discrimination of stiffness on silicone phantom tissue.

Index Terms—force and tactile sensing, fiber optics, tissue palpation, robotic palpation, medical robotics

I. INTRODUCTION

For robot hands to substitute human hands in tasks requiring tactile acuity, they should match the force and spatial

resolution of human fingertips while also having comparable stiffness and dimensions. Towards this goal, we present an approach for miniaturizing vision-based tactile sensors by using fiber bundles as optical conduits, demonstrating their use for manipulation tasks in constrained settings that cannot be done with larger fingers. An exemplar task is palpation through a natural orifice, as in the case of the digital rectal exam (DRE) for early prostate cancer screening [1]–[3].

II. DESIGN AND FABRICATION

As in early fiber-based imaging research [4], fiber bundles are used as conduits for illumination and imaging, decoupling the sensing element from supporting circuitry. Because the circuitry and processing are located remotely, the sensor size is no longer constrained by the packaging of an internal camera, lens, and lighting as in other such popular sensors [5]–[7]. Instead, the primary constraint is the bundle size, as determined by the desired resolution and lighting requirements.

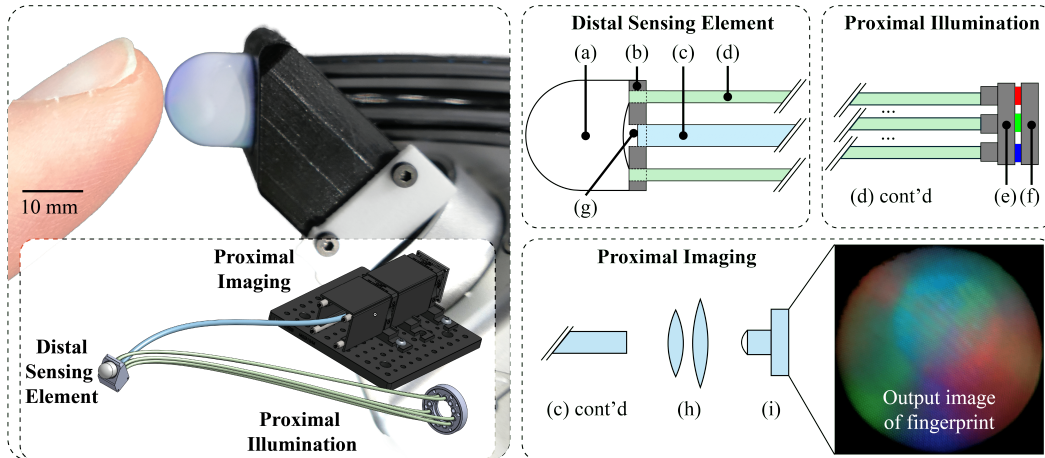


Fig. 1: DIGIT Pinki consists of: a distal sensing element, a proximal imaging system, and a proximal illumination system, connected with optical fiber bundles. The distal end contains (a) an elastomer gel mounted in (b) a 3D-printed housing. Both the (c) imaging and (d) illumination bundles mate to the gel. At the proximal end, the illumination bundles mate to the (e) collimator coupled to (f) LEDs. When making contact with an object (e.g. a woman's index finger), the gel is first imaged with (g) a distal hyperfocal lens, conveyed through the imaging fiber bundle, then magnified by (h) optical lenses and captured by the (i) camera. The proximal imaging and illumination may be co-located or separate.

TABLE I: Comparison between DIGIT and DIGIT Pinki

Sensor	Sensing Area (mm ²)	Sample Rate (Hz)	Spatial Resolution (mm)	Normal Force Resolution (N)	Shear Force Resolution (N)
DIGIT	304	60	0.150	0.006	0.012
DIGIT Pinki	1,404*	10**	0.22	0.005	0.005

* This number is from a proposed hyperfisheye lens design.

** Sampling rate at highest resolution of 4656x3496 pixels. A 30 Hz sampling rate is available at lower resolutions (1920x1080 pixels).

We guide the design with three requirements:

- small elastomer sensing element with diameter and stiffness comparable to a human fingertip,
- high spatial resolution for computer vision,
- high field of view across the curved fingertip area.

Based on these requirements, we construct a proof-of-concept prototype that is 15 mm in diameter, as shown in Fig. 1, achieving approximately the size of an adult female index fingertip or a fifth percentile male fingertip [8]. A detailed manufacturing guide can be found at <https://github.com/facebookresearch/digit-design>.

To assemble the sensor, we bond a hemispherical gel to a thin 3D-printed thread using Smooth-On Sil-Poxy Silicone Adhesive, and then screw the gel onto a 3D-printed housing. The housing is customizable; we show a housing compatible with the Allegro Hand. The “screw-on” gel allows easy swapping of tips, a useful feature for medical applications enabled by the fiber-based design.

We use a 7,400 core coherent fiber bundle as the imaging conduit, and 48-core incoherent fiber bundles as the illumination conduits. Illumination fibers were adhered with cyanoacrylate to a 3D-printed collimator directly coupled to a 12-LED Adafruit Neopixel ring mounted in an LED holder. To image the proximal end face of the imaging fiber bundle, we aligned an adjustable diopter, a 10x Plan microscope objective, and a microscope eyepiece to a 16MP IMX298 USB camera connected to a computer.

III. SENSOR CHARACTERIZATION

We assess force estimation by evaluating DIGIT Pinki’s ability to measure applied normal and shear forces at a contact. Because we are motivated by a tissue palpation use case, or other similar fine manipulation, we are primarily interested in the ability to measure light forces up to 1 N.

To collect training data, we mounted DIGIT Pinki on a Mecha robotic arm and installed a metal indenter probe on a force sensor on top of a linear stage. The ground truth normal and shear forces are synchronously collected with the images from the DIGIT Pinki for light normal forces up to 1 N and shear forces up to 100 mN, resulting in 100,000 image-force pairs with three different indenter types (4 mm, 12 mm diameter, and flat) for training a ResNet-18 model with mean square error as the training loss.

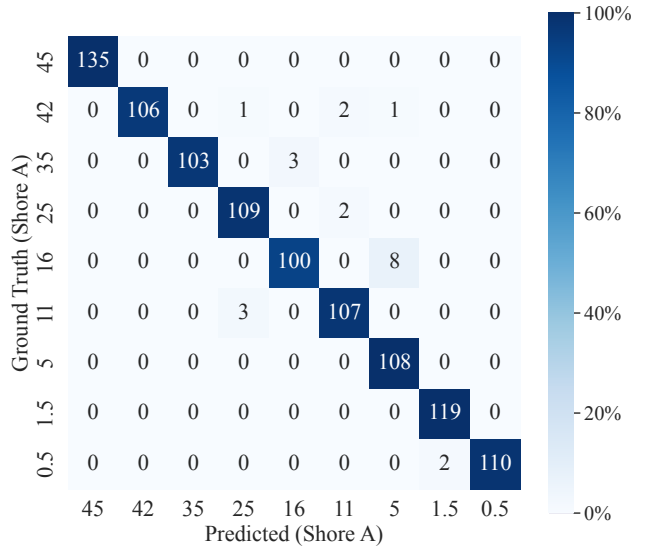


Fig. 2: Classifier performance on silicone hardness class prediction task. Prediction results on the silicone hardness samples show that the learned model is capable of predicting the hardness of the samples being touched with high accuracy.

Normal and shear force resolution are reported in Table I. DIGIT Pinki is able to accurately estimate light normal and shear forces over the elastomer tip. There is no significant difference in performance between the different indenter probe sizes, suggesting that DIGIT Pinki would perform well over a variety of contact sizes.

IV. PALPATION EXPERIMENTAL RESULTS

To be useful for medical palpation, we desire the ability to classify firmness over a range of values that simulate healthy and unhealthy tissue. We prepared a custom dataset associating stiffness (defined as hardness values on the Shore durometer scale for elastomers) to silicone samples of different relevant geometries. Using this dataset, we trained a classification model that classifies the hardness values based on a sequence of 16 image frames, in order to show DIGIT Pinki’s potential for palpation use cases.

We fine-tuned transformer-based video masked autoencoders (VideoMAE) [9]. The model takes as input the 16 frames sequences, and outputs a scalar that represents the hardness class. Results, plotted in the full confusion matrix (Fig. 2), show the model reaches 97.8% accuracy over 9 hardness classes. Based on these results, we see the trained model performs well in classifying elastomer hardness values that correspond to the range from healthy to unhealthy tissue.

ACKNOWLEDGMENT

This work was supported by Meta, the German Research Foundation, “Centre for Tactile Internet with Human-in-the-Loop” (CeTI) of TU Dresden, Zentrum für Informationsdienste und Hochleistungsrechnen (ZIH) of TU Dresden, Bundesministerium für Bildung und Forschung (BMBF) and German Academic Exchange Service (DAAD).

REFERENCES

- [1] L. Wang, B. Lu, M. He, Y. Wang, Z. Wang, and L. Du, "Prostate cancer incidence and mortality: global status and temporal trends in 89 countries from 2000 to 2019," *Frontiers in Public Health*, vol. 10, p. 176, 2022.
- [2] J. T. Wei, D. Barocas, S. Carlsson, F. Coakley, S. Eggener, R. Etzioni, S. W. Fine, M. Han, S. K. Kim, E. Kirkby *et al.*, "Early detection of prostate cancer: Aua/suo guideline part i: prostate cancer screening," *The Journal of Urology*, vol. 210, no. 1, pp. 46–53, 2023.
- [3] L. Naji, H. Randhawa, Z. Sohani, B. Dennis, D. Lautenbach, O. Kavanagh, M. Bawor, L. Banfield, and J. Profetto, "Digital rectal examination for prostate cancer screening in primary care: a systematic review and meta-analysis," *The Annals of Family Medicine*, vol. 16, no. 2, pp. 149–154, 2018.
- [4] S. Begej, "Planar and finger-shaped optical tactile sensors for robotic applications," *IEEE Journal on Robotics and Automation*, vol. 4, no. 5, pp. 472–484, 1988.
- [5] M. Lambeta, P.-W. Chou, S. Tian, B. Yang, B. Maloon, V. R. Most, D. Stroud, R. Santos, A. Byagowi, G. Kammerer *et al.*, "Digit: A novel design for a low-cost compact high-resolution tactile sensor with application to in-hand manipulation," *IEEE Robotics and Automation Letters*, vol. 5, no. 3, pp. 3838–3845, 2020.
- [6] W. Yuan, S. Dong, and E. H. Adelson, "Gelsight: High-resolution robot tactile sensors for estimating geometry and force," *Sensors*, vol. 17, no. 12, p. 2762, 2017.
- [7] N. F. Lepora, "Soft biomimetic optical tactile sensing with the tactip: A review," *IEEE Sensors Journal*, vol. 21, no. 19, pp. 21 131–21 143, 2021.
- [8] J. W. Garrett, "The adult human hand: some anthropometric and biomechanical considerations," *Human factors*, vol. 13, no. 2, pp. 117–131, 1971.
- [9] Z. Tong, Y. Song, J. Wang, and L. Wang, "Videomae: Masked autoencoders are data-efficient learners for self-supervised video pre-training," *Advances in neural information processing systems*, vol. 35, pp. 10 078–10 093, 2022.